Journal of Medicinal Chemistry

Brief Article

pubs.acs.org/jmc

Fragment-Based and Structure-Guided Discovery and Optimization of Rho Kinase Inhibitors

Rongshi Li,*[,†] Mathew P. Martin,[†] Yan Liu,[†] Binglin Wang,[†] Ronil A. Patel,[†] Jin-Yi Zhu,[†] Nan Sun,[†] Roberta Pireddu,[†] Nicholas J. Lawrence,[†] Jiannong Li,[‡] Eric B. Haura,[‡] Shen-Shu Sung,[§] Wayne C. Guida,[†] Ernst Schonbrunn,[†] and Said M. Sebti[†]

[†]Department of Drug Discovery and [‡]Department of Experimental Therapeutics, H. Lee Moffitt Cancer Center and Research Institute, 12902 Magnolia Drive, Tampa, Florida 33612, United States

Supporting Information

ABSTRACT: Using high concentration biochemical assays and fragment-based screening assisted by structure-guided design, we discovered a novel class of Rho-kinase inhibitors. Compound **18** was equipotent for ROCK1 (IC_{50} = 650 nM) and ROCK2 (IC_{50} = 670 nM), whereas compound **24** was more selective for ROCK2 (IC_{50} = 100 nM) over ROCK1 (IC_{50} = 1690 nM). The crystal structure of the compound **18**−ROCK1 complex revealed that **18** is a type 1 inhibitor that binds the hinge region in the ATP binding site. Compounds **18** and **24** inhibited potently the phosphorylation of the ROCK substrate MLC2 in intact human breast cancer cells.

INTRODUCTION

Fragment-based drug discovery (FBDD) is a powerful tool and a promising strategy in drug discovery. This approach is now an established paradigm, and success stories of fragment-based drug design and discovery have been reported for enzyme inhibitors as well as protein−protein interaction disruptors as anticancer therapeutics.[1] FBDD is based on screening small numbers (up to several thousands) of compounds to find low-affinity fragments with K_d values in the high micromolar to millimolar range. By contrast, conventional high-throughput screening (HTS) attempts to evaluate as many compounds as possible (often a million or more) in the hope of finding relatively more potent hits with K_d values of 10 μM or less. The advantages of fragment-based screening include accessing larger chemical space than classical HTS and avoiding steric clash to the target of interest from the larger molecules in traditional HTS. Chemical space has been estimated to be greater than 10^{60} molecules with 30 or fewer heavy (nonhydrogen) atoms.[2] However, when stereochemistry is not considered, there are 26 million synthetically accessible molecules with 11 or fewer heavy atoms composed of only first-row elements (C, N, O, and F).[3] Only a very small fraction of this chemical space can be explored by HTS. FBDD sets out to identify a starting point by screening a library of small molecules representing fragments that cover a larger chemical space of druglike matter. Therefore, high hit rates, more efficient hits, and the ability to sample chemical diversity more easily are expected from fragment-based screening. In addition, compounds derived from fragments tend to have better physicochemical properties.

The majority of fragment-based screening examples have relied upon biophysical techniques such as protein nuclear magnetic resonance (NMR),[1] X-ray crystallography,[4] surface plasmon resonance (SPR),[5] isothermal titration calorimetry (ITC),[6] target immobilized NMR screening (TINS),[7] native mass spectrometry (NMS),[8] and weak affinity chromatography (WAC).[9] Conventional biochemical assays for fragment-based screening have not been utilized frequently due to the limitation of method sensitivity and the concern that screening of fragments at high micromolar concentrations results in increased false-positive and false-negative rates. At the time we started our fragment-based discovery of Rho kinase (ROCK) inhibitors, there was virtually no report of using biochemical assays for fragment-based screening. However, there have been several recent reports describing the use of biochemical assays to screen fragments at high concentrations for hit identification successfully. These include the discovery of aminoindazole PDK1 inhibitors,[10] novel nonpeptidic inhibitors of β-secretase (BACE1),[11] inhibitors of checkpoint kinase 1,[12] and Hsp90 inhibitors.[13] In this manuscript, we have successfully used FBDD approaches and identified potent, selective, and cell-active inhibitors of ROCK1 and -2, enzymes involved in several pathological conditions such as cardiovascular diseases, glaucoma, inflammatory disorders, and cancer (see reviews[14−18]).

RESULTS AND DISCUSSION

We initiated our studies with a small fragment library containing seven compounds with pyridyl group as a potential "hinge" binder to ROCKs. Their molecular masses range from 199 to 293 Da. As shown in Table 1, coupling of *para*-aminopyridine with nicotinic acid, picolinic acid, isonicotinic acid, 4-chloronicotinic acid, and 5-bromonicotinc acid using *N*-ethyl-*N*′-(3-dimethylaminopropyl)carbodiimide (EDC) in *N*,*N*-dimethylformamide (DMF) yielded the corresponding amides (**1**−**5**). A *para*-fluorophenyl group was installed within compound **4** and **5** via a Suzuki reaction to give rise to **6** and **7**, respectively. This small fragment library was subjected to high concentration (400 μM) biochemical assays to determine

Received: September 29, 2011
Published: January 24, 2012

Table 1. Synthesis of Fragments 1−7 and IC_{50} and LE Values

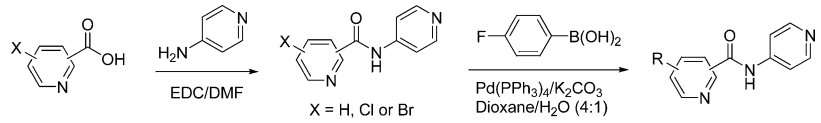

1: R = H, picolinamide **2:** R = H, isonicotinamide **3:** R = H, nicotinamide **4:** R = 4-Cl, nicotinamide
5: R = 5-Br, nicotinamide **6:** R = 4-(*para*-fluorophenyl), nicotinamide **7:** R = 5-(*para*-fluorophenyl), nicotinamide

compd	MW	ROCK1 (IC_{50}, μM)[a]	LE	ROCK2 (IC_{50}, μM)[a]	LE
1	199.21	35% inhibition[b]		35% inhibition[b]	
2	199.21	44% inhibition[b]		42% inhibition[b]	
3	199.21	75.5 ± 18.9	0.37	55.9 ± 11.3	0.39
4	233.65	72.5 ± 6.8	0.35	221.4 ± 25.7	0.31
5	278.10	270.0 ± 51.0	0.30	357.2 ± 35.3	0.29
6	293.30	>400	<0.2	>400	<0.2
7	293.30	>400	<0.2	>400	<0.2

[a]Data from triplicate experiments. [b]Compound concentration at 400 μM.

Table 2. Synthesis of Fragments and Compounds 8−19 and IC_{50} and LE Values

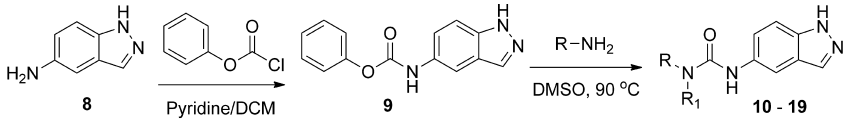

10: R = R_1 = Me **11:** R_1 = H, R = Ph **12:** R_1 = H, R = Bn **13:** R_1 = Me, R = $PhCH_2CH_2$

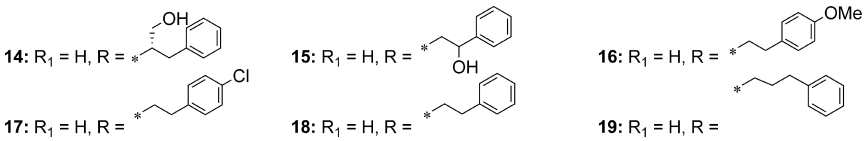

compd	MW	ROCK1 (IC_{50}, μM)[a]	LE	ROCK2 (IC_{50}, μM)[a]	LE
8	133.06	181.3 ± 50.7	0.51	119.7 ± 20.3	0.53
9	253.26	ND[b]		ND[b]	
10	204.10	59.1 ± 15.2	0.38	36.1 ± 5.9	0.40
11	252.10	157.1 ± 34.1	0.27	61.8 ± 9.6	0.30
12	266.12	13.9 ± 8.7	0.33	5.5 ± 3.1	0.36
13	294.15	21.5 ± 7.3	0.27	7.5 ± 1.7	0.32
14	310.14	4.6 ± 2.1	0.31	2.3 ± 0.6	0.33
15	296.13	2.9 ± 0.8	0.34	1.5 ± 0.4	0.36
16	310.14	2.6 ± 0.6	0.33	0.8 ± 0.3	0.36
17	314.09	2.2 ± 1.0	0.35	1.1 ± 0.3	0.37
18	280.13	0.65 ± 0.03	0.40	0.67 ± 0.12	0.40
19	294.15	2.46 ± 0.55	0.35	1.07 ± 0.14	0.37

[a]Data from triplicate experiments. [b]Not determined.

their in vitro inhibitory activities against ROCK1 and ROCK2 kinases. While both picolinamide (**1**) and isonicotinamide (**2**) showed only 30−40% inhibition on both ROCK1 and ROCK2 at 400 μM, nicotinamide (**3**) had IC_{50} values of 75.5 and 55.9 μM for ROCK1 and ROCK2, with ligand efficiencies (LE ≈ $-\Delta G$/HAC, defined as the free energy of binding divided by the number of nonhydrogen/heavy atoms[19]) of 0.37 and 0.39, respectively. 4-Chlorosubsituted nicotinamide (**4**) decreased the inhibitory activity against ROCK2 by 4-fold. 5-Bromosubstituted nicotinamide (**5**) decreased ROCK1 and ROCK2 inhibitory activities by up to 6-fold. Larger substituent (*para*-fluorophenyl) at the corresponding positions (**6** and **7**) diminished the activity even further (Table 1). These results suggest that the fragments (**4**−**7**) bearing bulkier functional group in the 4- or 5-position of nicotinamide may interfere with their binding to the hinge region due to steric clashes. This led us to evaluate other hinge binders to circumvent this potential problem.

5-Aminoindazole (**8**) was chosen as a substitute fragment for *para*-aminopyridine. The distances from the amino nitrogen to 1-indazole nitrogen and 2-indazole nitrogen are 5.5 and 5.9 Å, respectively, whereas the distance from the *para*-amino nitrogen to pyridine nitrogen is only 4.2 Å. Fragment **8** showed IC_{50} values of 181 μM for ROCK1 and 120 μM against ROCK2 with LE being 0.51 and 0.53, respectively (Table 2). Although *N*-(1*H*-indazole-5-yl)acetamide demonstrated improved potency (65 μM for ROCK1 and 40 μM for ROCK2), the amides derived from the corresponding aromatic carboxylic acids did not yield potency-improved compounds (data not shown). This finding led us to identify an extended linker. As shown in Table 2, dimethyl/indazole urea **10** had improved potency with IC_{50} values of 59 μM for ROCK1 and 36 μM against ROCK2 with LEs being 0.38 and 0.40,

dx.doi.org/10.1021/jm201289r | J. Med. Chem. 2012, 55, 2474−2478

Table 3. Synthesis of Compounds 20−27 and IC_{50} and LE Values

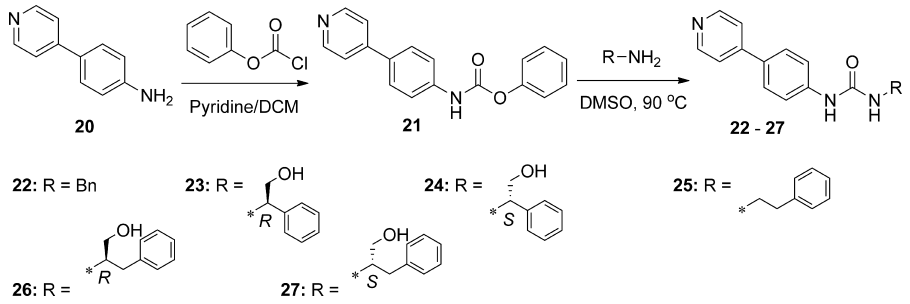

compd	MW	ROCK1 (IC_{50}, μM)[a]	LE	ROCK2 (IC_{50}, μM)[a]	LE
22	303.14	1.15 ± 0.41	0.35	0.26 ± 0.07	0.39
23	333.15	9.07 ± 2.52	0.28	7.52 ± 1.51	0.28
24	333.15	1.69 ± 0.17	0.31	0.10 ± 0.03	0.38
25	317.15	2.61 ± 0.41	0.32	19.80 ± 3.29	0.27
26	347.16	1.41 ± 0.50	0.31	5.36 ± 0.94	0.28
27	347.16	31.01 ± 10.51	0.24	32.92 ± 4.67	0.23

[a]Data from triplicate experiments.

respectively. However, substitution of one of the methyl groups by a phenyl group and the other with a hydrogen (compound **11**) diminished activity. The addition of a methylene moiety between the urea nitrogen and the phenyl group of **11** resulted in compound **12** (IC_{50} = 14 μM and 5.5 μM for ROCK1 and ROCK2, respectively) with over an 11-fold improvement in potency. Compound **12** was reported as a ROCK2 inhibitor with an IC_{50} value of 260 nM along with three other analogues of chloro- or fluoro-substituted phenyl groups.[20,21] The 20−50-fold difference in IC_{50} values between our compound **12** and those reported[20] is likely due to different assay conditions, that is, the enzyme or ATP concentrations, and our emphasis is relative activity. Because no compounds with a two carbon spacer between the urea nitrogen and the phenyl group have previously been reported, we then designed and synthesized six novel compounds with a two carbon spacer (**13**−**18**). Compound **18** showed an IC_{50} of 650 and 670 nM for ROCK1 and ROCK2, respectively, with a 21- and 242-fold improvement in potency (ROCK1) over compounds **12** and **11**, respectively (Table 2), suggesting that the ethylene linker distance allowed the phenyl group to reach a deep hydrophobic pocket within the enzyme binding site of ROCK. However, compound **19** with a three carbon spacer decreased the inhibitory activities by 3.8-fold for ROCK1 and 1.6-fold for ROCK2, respectively (IC_{50} = 2.46 and 1.07 μM for ROCK1 and ROCK2) with decreased LEs, suggesting that the ethylene linker in **18** is the optimal spacer in this series. The addition of methylenehydroxyl group to the ethylene as in **14** and hydroxyl group to the ethylene in **15** or the addition of a methoxy or a chloro to the phenyl ring as in **16** and **17** all diminished the potency of **18** to varying degrees, further confirming the hydrophobicity of the binding pocket. Replacement of the urea hydrogen atom of **18** with a methyl group gave rise to the much less potent compound **13**, possibly due to the lack of essential free hydrogen on one of the urea nitrogen atoms.

Compounds **10**−**19** were synthesized from commercially available **8** via a common intermediate **9**, by reacting **8** with phenylchloroformate in dichloromethane (DCM) to form an activated carbamate followed by displacement by the corresponding amines.

A molecular modeling study of a docked structure **18** into ROCK1 (PDB code: 2ESM)[22] suggested that potential hydrogen-bonding interactions can be formed between amino acid residues in the hinge region and **18**. As shown in Figure 1a in the Supporting Information, potential hydrogen-bonding interactions are postulated between the indazole nitrogen and the amide NH from M156, the indazole NH, and the carbonyl O from E154 (this binding mode is consistent with that of a cocrystal complex of a reported indazole-containing ROCK1 inhibitor[23]) and one of the urea NH and carboxylic O from D216 of the DGF motif. However, R84, which is in close proximity, was not utilized. To explore the possibility of this additional hydrogen bonding, we considered a new fragment 4-(pyridine-4-yl)aniline **20** as a surrogate of indazole **8**. The distance between the pyridyl nitrogen of **20** and the aniline nitrogen connecting to the urea linker is longer (8.5 Å) than that of **8** (5.9 Å). This shift may allow potential hydrogen-bonding interactions with R84.

Six more compounds (**22**−**27**) with different spacers were synthesized via the same route as that for synthesis of **10**−**19** described above, and their kinase inhibitory activities were evaluated. By the time compounds **22**−**27** were synthesized, this pyridine series was published in a patent, and most recently, their anti-inflammatory activities as ROCK inhibitors appeared.[24] As shown in Table 3, compound **22** with a new hinge binder moiety, 4-(pyridine-4-yl)aniline, showed similar activity to that of **18** (Table 2). Compound **18** has a shorter hinge binder (aminoindazole) but a longer spacer (ethylene) while compound **22** has a longer hinge binder (pyridylaniline) but a shorter spacer (methylene). Their in vitro activities against ROCK1 and ROCK2 are from submicromolar to a micromolar (ROCK1, 0.65 μM for **18** and 1.15 μM for **22**; ROCK2, 0.67 μM for **18** and 0.26 μM for **22**; see Tables 2 and 3). As shown in Figure 1b in the Supporting Information, compound **22** was docked in the same ATP binding pocket as that of **18**. While the hydrogen-bonding interaction with M156 is retained for **22**, the interactions with E154 and D216 are lost. New hydrogen-bonding interactions can be achieved between the urea (NH and O) of **22** and R84.

Most recently, we cocrystallized compound **18** with the kinase domain of human ROCK1 (residues 6−415) to

dx.doi.org/10.1021/jm201289r | J. Med. Chem. 2012, 55, 2474−2478

experimentally determine the mode of action of our novel indazole-containing ROCK1 inhibitor series. The ROCK1−**18** complex crystallized in space group $C222_1$ with two dimers per asymmetric unit. The structure was refined to 2.3 Å resolution with R_{cryst} and R_{free} values of 18.8 and 23.6%, respectively (Table 1 in the Supporting Information). The inhibitor binds to the ATP site of ROCK1 essentially as predicted by molecular docking (Figure 1c). The indazole nitrogen atoms establish

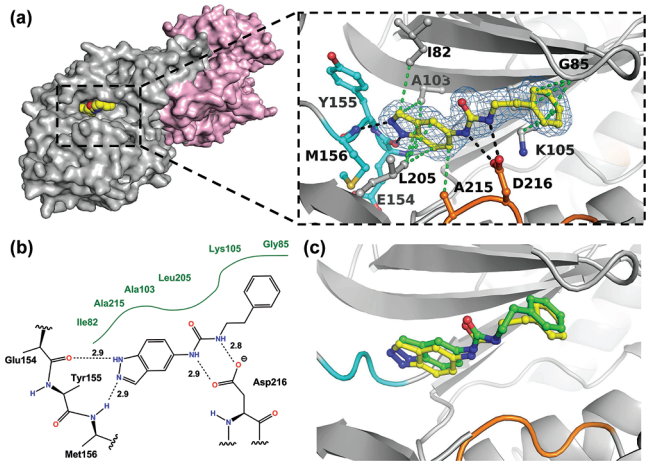

Figure 1. Molecular mode of action of compound **18**. (a) Surface presentation of the ROCK1 dimer in complex with **18** determined by X-ray crystallography at 2.3 Å resolution. Exploded view detailing the binding interactions of **18** (yellow) within the ATP site; the hinge and DFG regions are indicated in cyan and orange, respectively. Displayed in blue is the $2F_o - F_c$ electron density, contoured at 1σ around the inhibitor. Potential hydrogen-bonding and van der Waal interactions are shown as black and green dotted lines, respectively. (b) Schematic presentation of the binding interactions between **18** and the ATP site. (c) Overlay of compound **18** in the active site of ROCK1 determined by X-ray crystallography (yellow) and predicted by molecular modeling (green).

hydrogen-bonding interactions with the main chain of residues Met156 and Glu154 of the hinge region. In addition, the indazole ring establishes a series of van der Waals (hydrophobic) interactions with Ile82, Ala215, Ala103, and Leu205 (Figure 1b). The urea linker interacts with the side chain of Asp216 of the DFG motif. The phenyl ring is sandwiched between the P loop (Arg84−Gly88) of the upper N-terminal lobe and the side chain of the catalytic residue Lys105 (Figure 1a). The crystal structure corroborates the results from the molecular modeling studies, and only small changes are observed in the conformation of the inhibitor molecule.

Two pairs of chiral spacers were chosen to probe possible stereochemical preferences that may exist in the enzyme binding site. Compound **24** with an *S*-configuration (IC_{50} = 100 nM) showed 75-fold more kinase inhibitory activity than compound **23** with a *R*-configuration (IC_{50} = 7520 nM) for ROCK2, while the difference is only 5-fold for ROCK1 (IC_{50} = 9.07 μM for **23** vs 1.69 μM for **24**). However, their corresponding homologues with an additional methylene spacer exhibited the opposite selectivity. While compound **26** with a *R*-configuration is only 6-fold more active than that of **27** with an *S*-configuration toward ROCK2 (IC_{50} = 5.36 μM for **26** vs 32.92 μM for **27**), 22-fold more inhibitory activity toward ROCK1 is observed (IC_{50} = 1.41 μM for **26** vs 31.01 μM for **27**). In addition, compound **26** demonstrated 4-fold selectivity for ROCK1 over ROCK2. Eight-fold selectivity of ROCK1 over ROCK2 is also observed for compound **25** with ethylene spacer (Table 3).

The in vitro kinase SAR yielded potent and selective ROCK inhibitors. We next determined whether some of these are capable of entering intact cells, reaching their target and inhibiting ROCK from phosphorylating its substrate MLC2. To this end, we discovered that compound **18** and **24** inhibited potently the phosphorylation of the ROCK substrate MLC2 in intact human breast cancer cells as described in the Supporting Information.

■ CONCLUSION

Recent studies identified ROCK inhibitors as potential therapies for pathological conditions such as glaucoma.[14−19] None of these studies have used FBDD approaches except for the identification of a ROCK1 inhibitor from a historical thrombin/FactorXa building block by fragment-based NMR screening.[25,26] In this study, using high concentration biochemical assays and fragment-based screening, we have discovered fragments to inhibit Rho-associated kinases. We also demonstrated the design and optimization of ROCK inhibitors using LE as a general guide to assess the binding potential of the fragments and to guide the optimization process. Molecular modeling aided the design and fragment hopping from one hinge binder to another for the optimization of ROCK inhibitors. Our structural biology studies yielded an X-ray cocrystal of ROCK1−compound **18** in 2.3 Å resolution and, coupled with molecular modeling studies, provided the molecular basis for the design of more potent and selective ROCK inhibitors. Optimization of fragments yielded potent (100 nM) ROCK inhibitors that inhibited in intact human cancer cells at low micromolar concentration the phosphorylation of MLC2, a ROCK substrate, but not the phosphorylation of proteins that are not substrates of ROCK such as Erk1/2. Future studies will focus on determining the ability of the most potent inhibitors to suppress migration and invasion, cancer hallmarks known to be mediated by ROCK.

■ EXPERIMENTAL SECTION

The synthesis of fragments and ROCK inhibitors, molecular modeling, X-ray cocrystallography, Z-lyte assays for determining ROCK kinase activities, and effects of ROCK inhibitors on the phosphorylation levels of MLC2 (a ROCK substrate) and Erk1/2 (not a ROCK substrate) in human cancer cells are reported in the Supporting Information.

■ ASSOCIATED CONTENT

Ⓢ Supporting Information

Preparation of compounds **1**−**27**, ^{1}H NMR, HRMS, HPLC purity, Z-lyte assays, and effects of our ROCK inhibitors in human cancer cells, molecular modeling, and X-ray cocrystallography. This material is available free of charge via the Internet at http://pubs.acs.org.

■ AUTHOR INFORMATION

Corresponding Author

*Tel: 813-745-6485. Fax: 813-745-6875. E-mail: Rongshi.Li@moffitt.org.

Present Address

§Department of Pharmacology, Penn State College of Medicine, Hershey, Pennsylvania 17033.

■ ACKNOWLEDGMENTS

This work was supported partially by startup funds (R.L.), 5U19CA067771-15 (S.M.S). We thank the Moffitt Chemical Biology Core facility for high concentration fragment-based screening. We thank Drs. Bi-Cheng Wang and Lirong Chen at the University of Georgia for the kind support during usage of Beamline 22-ID, SER-CAT.

■ ABBREVIATIONS USED

FBDD, fragment-based drug discovery; HTS, high-throughput screening; NMR, nuclear magnetic resonance; SPR, surface plasmon resonance; ITC, isothermal titration calorimetry; TINS, target immobilized NMR screening; NMS, native mass spectrometry; WAC, weak affinity chromatography; ROCK, Rho kinase; EDC, *N*-ethyl-*N*′-(3-dimethylaminopropyl)-carbodiimide; DMAP, 4-*N*,*N*-dimethylaminopyridine; DMF, *N*,*N*-dimethylformamide; LE, ligand efficiency; DCM, dichloromethane

■ REFERENCES

(1) Hajduk, P. J.; Greer, J. A decade of fragment-based drug design: strategic advances and lessons learned. *Nat. Rev. Drug Discovery* **2007**, *6*, 211−219.

(2) Bohacek, R. S.; McMartin, C.; Guida, W. C. The art and practice of structure-based drug design: a molecular modeling perspective. *Med. Res. Rev.* **1996**, *16*, 3−50.

(3) Fink, T.; Reymond, J. L. Virtual exploration of the chemical universe up to 11 atoms of C, N, O, F: assembly of 26.4 million structures (110.9 million stereoisomers) and analysis for new ring systems, stereochemistry, physicochemical properties, compound classes, and drug discovery. *J. Chem. Inf. Model.* **2007**, *47*, 342−353.

(4) Jhoti, H.; Cleasby, A.; Verdonk, M.; Williams, G. Fragment-based screening using X-ray crystallography and NMR spectroscopy. *Curr. Opin. Chem. Biol.* **2007**, *11*, 485−493.

(5) Navratilova, I.; Hopkins, A. L. Fragment Screening by Surface Plasmon Resonance. *ACS Med. Chem. Lett.* **2010**, *1*, 44−48.

(6) Ladbury, J. E.; Klebe, G.; Freire, E. Adding calorimetric data to decision making in lead discovery: a hot tip. *Nat. Rev. Drug Discovery* **2010**, *9*, 23−27.

(7) Siegal, G.; Hollander, J. G. Target immobilization and NMR screening of fragments in early drug discovery. *Curr. Top. Med. Chem.* **2009**, *9*, 1736−1745.

(8) Hannah, V. V.; Atmanene, C.; Zeyer, D.; Dorsselaer, A. V.; Sanglier-Cianférani, S. Native MS: An 'ESI, way to support structure- and fragment-based drug discovery. *Future Med. Chem.* **2010**, *2*, 35−50.

(9) Duong-Thi, M. D.; Meiby, E.; Bergstrom, M.; Fex, T.; Isaksson, R.; Ohlson, S. Weak affinity chromatography as a new approach for fragment screening in drug discovery. *Anal. Biochem.* **2011**, *414*, 138−146.

(10) Medina, J. R.; Blackledge, C. W.; Heerding, D. A.; Campobasso, N.; Ward, P.; Briand, J.; Wright, L.; Axten, J. M. Aminoindazole PDK1 Inhibitors: A Case Study in Fragment-Based Drug Discovery. *ACS Med. Chem. Lett.* **2010**, *1*, 439−442.

(11) Godemann, R.; Madden, J.; Kramer, J.; Smith, M.; Fritz, U.; Hesterkamp, T.; Barker, J.; Hoppner, S.; Hallett, D.; Cesura, A.; Ebneth, A.; Kemp, J. Fragment-based discovery of BACE1 inhibitors using functional assays. *Biochemistry* **2009**, *48*, 10743−10751.

(12) Matthews, T. P.; Klair, S.; Burns, S.; Boxall, K.; Cherry, M.; Fisher, M.; Westwood, I. M.; Walton, M. I.; McHardy, T.; Cheung, K. M.; Van Montfort, R.; Williams, D.; Aherne, G. W.; Garrett, M. D.; Reader, J.; Collins, I. Identification of inhibitors of checkpoint kinase 1 through template screening. *J. Med. Chem.* **2009**, *52*, 4810−4819.

(13) Barker, J. J.; Barker, O.; Boggio, R.; Chauhan, V.; Cheng, R. K.; Corden, V.; Courtney, S. M.; Edwards, N.; Falque, V. M.; Fusar, F.; Gardiner, M.; Hamelin, E. M.; Hesterkamp, T.; Ichihara, O.; Jones, R. S.; Mather, O.; Mercurio, C.; Minucci, S.; Montalbetti, C. A.; Muller, A.; Patel, D.; Phillips, B. G.; Varasi, M.; Whittaker, M.; Winkler, D.; Yarnold, C. J. Fragment-based identification of Hsp90 inhibitors. *ChemMedChem* **2009**, *4*, 963−966.

(14) Dong, M.; Yan, B. P.; Liao, J. K.; Lam, Y. Y.; Yip, G. W.; Yu, C. M. Rho-kinase inhibition: A novel therapeutic target for the treatment of cardiovascular diseases. *Drug Discovery Today* **2010**, *15*, 622−629.

(15) LoGrasso, P. V.; Feng, Y. Rho kinase (ROCK) inhibitors and their application to inflammatory disorders. *Curr. Top. Med. Chem.* **2009**, *9*, 704−723.

(16) Micuda, S.; Rosel, D.; Ryska, A.; Brabek, J. ROCK inhibitors as emerging therapeutic candidates for sarcomas. *Curr. Cancer Drug Targets* **2010**, *10*, 127−134.

(17) Yang, X.; Zhang, Y.; Wang, S.; Shi, W. Effect of fasudil on growth, adhesion, invasion, and migration of 95D lung carcinoma cells in vitro. *Can. J. Physiol. Pharmacol.* **2010**, *88*, 874−879.

(18) Kidera, Y.; Tsubaki, M.; Yamazoe, Y.; Shoji, K.; Nakamura, H.; Ogaki, M.; Satou, T.; Itoh, T.; Isozaki, M.; Kaneko, J.; Tanimori, Y.; Yanae, M.; Nishida, S. Reduction of lung metastasis, cell invasion, and adhesion in mouse melanoma by statin-induced blockade of the Rho/Rho-associated coiled-coil-containing protein kinase pathway. *J. Exp. Clin. Cancer Res.* **2010**, *29*, 127.

(19) Hajduk, P. J. Fragment-based drug design: How big is too big? *J. Med. Chem.* **2006**, *49*, 6972−6976.

(20) Iwakubo, M.; Takami, A.; Okada, Y.; Kawata, T.; Tagami, Y.; Ohashi, H.; Sato, M.; Sugiyama, T.; Fukushima, K.; Iijima, H. Design and synthesis of Rho kinase inhibitors (II). *Bioorg. Med. Chem.* **2007**, *15*, 350−364.

(21) Takami, A.; Iwakubo, M.; Okada, Y.; Kawata, T.; Odai, H.; Takahashi, N.; Shindo, K.; Kimura, K.; Tagami, Y.; Miyake, M.; Fukushima, K.; Inagaki, M.; Amano, M.; Kaibuchi, K.; Iijima, H. Design and synthesis of Rho kinase inhibitors (I). *Bioorg. Med. Chem.* **2004**, *12*, 2115−2137.

(22) Jacobs, M.; Hayakawa, K.; Swenson, L.; Bellon, S.; Fleming, M.; Taslimi, P.; Doran, J. The structure of dimeric ROCK I reveals the mechanism for ligand selectivity. *J. Biol. Chem.* **2006**, *281*, 260−268.

(23) Sehon, C. A.; Wang, G. Z.; Viet, A. Q.; Goodman, K. B.; Dowdell, S. E.; Elkins, P. A.; Semus, S. F.; Evans, C.; Jolivette, L. J.; Kirkpatrick, R. B.; Dul, E.; Khandekar, S. S.; Yi, T.; Wright, L. L.; Smith, G. K.; Behm, D. J.; Bentley, R.; Doe, C. P.; Hu, E.; Lee, D. Potent, selective and orally bioavailable dihydropyrimidine inhibitors of Rho kinase (ROCK1) as potential therapeutic agents for cardiovascular diseases. *J. Med. Chem.* **2008**, *51*, 6631−6634.

(24) Yoshimi, E.; Kumakura, F.; Hatori, C.; Hamachi, E.; Iwashita, A.; Ishii, N.; Terasawa, T.; Shimizu, Y.; Takeshita, N. Antinociceptive effects of AS1892802, a novel Rho kinase inhibitor, in rat models of inflammatory and noninflammatory arthritis. *J. Pharmacol. Exp. Ther.* **2010**, *334*, 955−963.

(25) Ray, P.; Wright, J.; Adam, J.; Bennett, J.; Boucharens, S.; Black, D.; Cook, A.; Brown, A. R.; Epemolu, O.; Fletcher, D.; Haunso, A.; Huggett, M.; Jones, P.; Laats, S.; Lyons, A.; Mestres, J.; de Man, J.; Morphy, R.; Rankovic, Z.; Sherborne, B.; Sherry, L.; van Straten, N.; Westwood, P.; Zaman, G. Z. Fragment-based discovery of 6-substituted isoquinolin-1-amine based ROCK-I inhibitors. *Bioorg. Med. Chem. Lett.* **2011**, *21*, 97−101.

(26) Ray, P.; Wright, J.; Adam, J.; Boucharens, S.; Black, D.; Brown, A. R.; Epemolu, O.; Fletcher, D.; Huggett, M.; Jones, P.; Laats, S.; Lyons, A.; de Man, J.; Morphy, R.; Sherborne, B.; Sherry, L.; Straten, N.; Westwood, P.; York, M. Optimisation of 6-substituted isoquinolin-1-amine based ROCK-I inhibitors. *Bioorg. Med. Chem. Lett.* **2011**, *21*, 1084−1088.